FREQUENCY-DEPENDENT BOUNDARY CONDITION
FOR THE 3-D DIGITAL WAVEGUIDE MESH

Antti Kelloniemi

Telecommunications Software and Multimedia laboratory
Helsinki University of Technology, Finland
antti.kelloniemi@panphonics.fi

ABSTRACT

The three-dimensional digital waveguide mesh is a method for modeling the propagation of sound waves in space. It provides a simulation of the state of the whole soundfield at discrete timesteps. The updating functions of the mesh can be formulated either using physical values of sound pressure or particle velocity, also called the Kirchhoff values, or using a wave decomposition of these instead. Computation in homogenous media is significantly lighter using Kirchhoff variables, but frequency-dependent boundary conditions are more easily defined with wave variables. In this paper a conversion method between these two variable types has been further simplified. Using the resulting structure, a novel method for defining the mesh boundaries with digital filters is introduced. With this new method, the reflection coefficients can be defined in a frequency-dependent manner at the boundaries of a Kirchhoff variable mesh. This leads to computationally lighter and more realistic simulations than previous solutions.

1. INTRODUCTION

The best method for room acoustic modeling depends on the frequencies of interest and size and complexity of the modeled space. At frequencies below the Schroeder frequency, the wave phenomena such as interference and diffraction of sound have to be taken into account [1]. Geometrical methods typically fail in this when non-trivial shapes are considered. In contrary, good results are accomplished by modeling the wave propagation and scattering in discrete time and space, for example with the digital waveguide (DWG) mesh method as presented in Section 2.

Digital waveguides have been widely used for musical sound synthesis [2, 3]. For example, in 1-D a DWG provides an effective model of a vibrating string. The method has been extended to the multi-dimensional case using the DWG mesh to provide models of vibrating membranes in 2-D [4, 5] and acoustic enclosures in 3-D [6, 7, 8].

The mesh scheme has two formulations: The computation can be done using traveling wave variables or Kirchhoff (*K*) variables [2, 6]. While these formulations are technically equivalent, one variable type is often better suited than the other for certain applications. When operating with multi-dimensional models, the traveling wave formulation consumes significantly more computational and memory resources than the finite-difference time-domain scheme with K variables. On the other hand, wave variables are needed when digital filters are designed for modeling frequency-dependent boundary conditions or air absorption, for example [9, 10]. The conversion between the two variable types was introduced by Karjalainen and Erkut [11]. A simplified KW-converter structure based on their results is introduced in Section 3.

The KW-converter makes it possible to define the reflection characteristics of the boundaries of a K variable mesh by digital filters. A small variation in its design enables use of a linear-phase FIR filter without adding extra delays compared to a single real valued reflection coefficient, as shown in Section 4. In this design, the filter coefficients are related to the reflection coefficient values in a very straightforward way. In Section 5, a case study is presented, where by use of this filter structure the T_{60} values of a modeled lecture hall are matched with measurement results.

Conclusion of the results and discussion of the future improvements end this paper in Section 6.

2. THE DIGITAL WAVEGUIDE MESH

2.1. The 1-D Digital Waveguides

In one dimension, a DWG is constructed of two delay lines passing the signal in opposite directions and of scattering junctions between them. With wave variables the value at a junction is calculated as a sum of incoming wave variable values p_l^+:

$$p_c(n) = \frac{2\sum_{l=1}^{2} Y_l p_l^+(n)}{\sum_{l=1}^{2} Y_l}, \tag{1}$$

and the outgoing wave variable values are then updated as:

$$p_l^-(n) = p_c(n) - p_l^+(n), \tag{2}$$

where p is the signal value at a junction, subscript c denotes the junction to be calculated, n is the time step index, Y is the characteristic admittance of an interconnection, and index l denotes the unit delays connected to the junction c [4]. The transformation from outgoing to ingoing values happens by passing the values through the unit delays at the interconnections.

In Kirchhoff variables, the updating of the 1-D junction may be written as:

$$p_c(n) = \frac{2\sum_{l=1}^{2} Y_l p_l(n-1)}{\sum_{l=1}^{2} Y_l} - p_c(n-2), \tag{3}$$

where index l runs now through the neighboring junctions instead of interconnections.

2.2. The 3-D Triangular Mesh

A multi-dimensional DWG structure is constructed by connecting multiple delay lines together. A DWG mesh is defined by a regular grid of scattering junctions separated by bi-directional unit delays. The grid can be constructed in many topologies. For this study, a 3-D triangular structure, also known as 3-D dodecahedral or hexagonal close packed structure[12, 13], was chosen as it
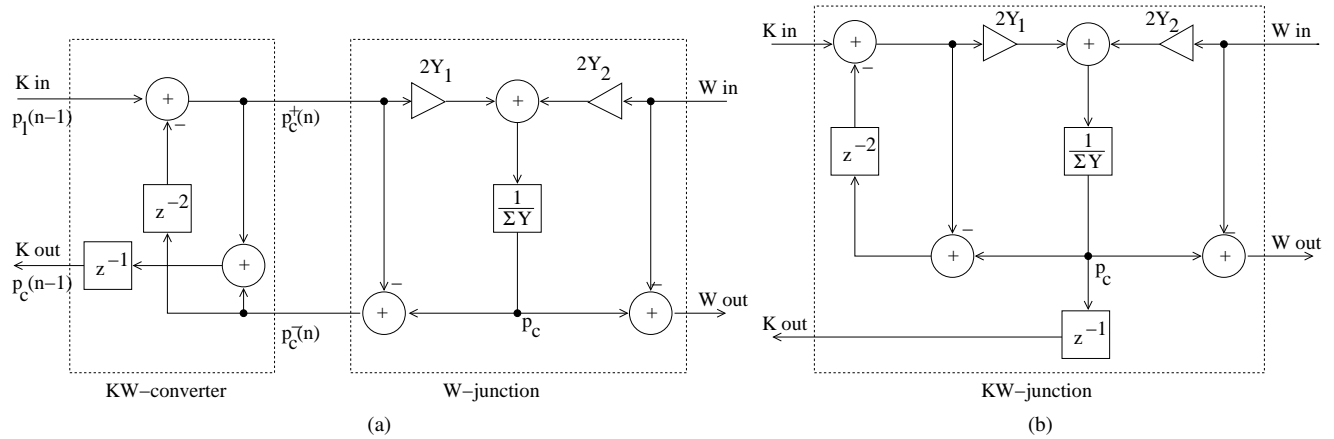
Figure 1: *(a) KW-converter: Filter block for changing between Kirchhoff (K) and traveling wave (W) variables is shown with a wave variable junction [11]. (b) KW-junction: The K to wave variable conversion is included at the K input of the junction, scattering computation is done with wave variables and K variable output is provided by delaying the junction value p_c by one time step.*

causes less numerical dispersion than the original rectilinear mesh and is more efficient in 3-D than for example the interpolated rectilinear mesh [14, 15].

Kirchhoff variables are used in the interior of the mesh for computational efficiency. When the mesh is considered to be homogenous, the updating function of a 3-D triangular scattering junction with 12 neighbors is written as

$$p_c(n) = \frac{2}{12}\sum_{l=1}^{12} p_l(n-1) - p_c(n-2). \qquad (4)$$

When the triangular topology is used, the maximum simulation frequency f is restricted to one third of the sampling frequency f_s of the mesh [16].

The nominal wave propagation speed in a DWG mesh is determined as

$$c = \frac{f_s \Delta x}{\sqrt{N}}, \qquad (5)$$

where Δx is the spatial step length and N is the number of spatial dimensions. In a 3-D mesh, wave speed is thus $c = \sqrt{1/3}$ spatial steps per time step [14, 17].

3. CONVERSION BETWEEN KIRCHHOFF AND TRAVELING WAVE VARIABLES

A converter between the two variable types in a digital waveguide mesh is a useful tool, as characteristics of both formulations are needed for creating efficient yet flexible models [10, 11]. Simple rules can be derived for the KW-conversion shown in Fig. 1(a). Firstly, a Kirchhoff variable $p_l(n-1)$ at the K input is converted into a traveling wave variable by $p_c^+(n) = p_l(n-1) - p_c^-(n-2)$. Secondly, for reverse conversion, the junction value p_c at current time instant n is calculated also in a wave variable mesh as shown in (1). An input for a neighboring K junction is created from this by passing the value through a unit delay.

A new kind of building block for mixed modeling, namely the KW-junction, is introduced in Fig. 1(b). Before summing with the wave variables, the K variables are filtered just as earlier and the wave variable ports are constructed as in pure wave variable junctions. More ports with their respective admittances and input

and output signals could be added. The novelty is that the K output is computed only once and not separately for each port as in Fig. 1(a). If the junction would have m K ports, m summations and $m-1$ unit delays would be saved by the new KW-junction in comparison to the use of earlier proposed KW-converter structure.

4. THE NEW BOUNDARY FILTER FOR K MESH

To approximate the behavior of the wavefront when it coincides with walls, furniture, or other boundaries, the mesh edges have to be defined in a controllable manner. For the K mesh, this has been possible only by defining simple real valued reflection coefficients. In contrary, the reflection characteristics of real walls are significantly frequency-dependent both in magnitude and in phase.

A new construction for defining the reflection coefficients for the K mesh is based on the structure shown in Fig. 1(b). At the boundary, only the K port on the left hand side of the junction is connected to the mesh and there is no signal connected to the wave variable port on the right hand side. The admittance of the K port Y_1 is the same as that of the homogenous mesh, and the reflection coefficient is defined by variable Y_2. Thus, from (3) we get

$$p_b(n) = \frac{2Y_1 p_1(n-1)}{Y_1 + Y_2} - p_b(n-2), \qquad (6)$$

where p_b is the value at the boundary junction and p_1 is the value at the neighboring junction inside the mesh.

The admittance value can be replaced with reflection coefficients: $Y_2 = (1-R)/(1+R)$. Using this, and if admittance Y_1 is normalized to 1, (6) can be written as

$$p_b(n) = (1+R)p_1(n-1) - p_b(n-2). \qquad (7)$$

In Fig. 2, the boundary junction structure is shown in a general form. It includes the conversion from K variables to wave variables and a boundary filter $H(z)$. It can be noted that when comparing with Fig. 1(b), one unit delay has been omitted from the signal line passing the signal to the first summation after K variable input and also from the K output line. The scheme is reorganized so that now this unit delay is implemented at the second vertical signal line from left and also inside the filter $H(z)$.
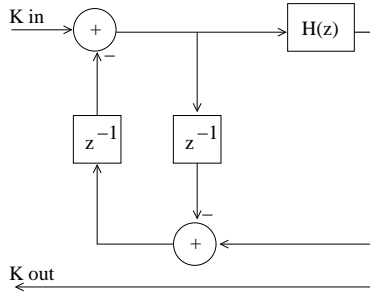
Figure 2: *The boundary filter for K mesh: Conversion to wave variables is performed by filtering the input signal. The location of a unit delay has been altered compared to the conversion block in Fig. 1(b) and the multiplications with admittance coefficients have been replaced with filter $H(z)$.*
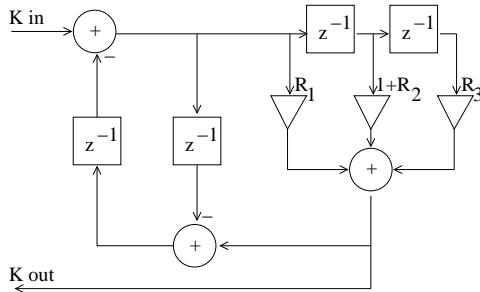

Figure 3: *The boundary filter for K mesh: A 3-tap FIR filter is realized as an example.*

If $H(z) = (1 + R)z^{-1}$, (7) is implemented with real-valued reflection coefficient R. The reflection coefficient should get values $-1 \le R \le 1$ for stable operation. Other possible filters include fractional delays for adjusting the boundary location [13], different lengths of delay lines for diffusive structures [18], or high-order IIR or FIR filters [9].

A very basic example for a boundary filter is shown in Fig. 3. The FIR filter with $H(z) = R_1 + (1 + R_2)z^{-1} + R_3z^{-2}$ causes no extra delay to the reflected signal if $R_1 = R_3$. With this kind of linear-phase filter, the boundary location in the model is not altered in comparison to the real valued reflection coefficient realization. The reflection coefficient value at DC and a simple lowpass or highpass behavior can be defined with the two free parameters of the filter.

More complex boundaries can be simulated using higher order FIR or IIR filters, for which the magnitude and the phase of the responses can be defined at all simulation frequencies.

5. APPLICATION: MODELING OF A LECTURE HALL

As a case study, the lecture hall T3 at Helsinki University of Technology was modeled and the results compared with measured responses. As shown in Fig. 4, the left side wall and the back wall are sloping. A soft absorbent plate is hung at 0.40 m below the ceiling, covering the full area from the back wall to 3.00 m from the front wall.

Boards and stools were present in the hall during the measurements. The sound source was located 2.70 m away from the left side wall and from the front wall equally, at a height of 1.20 m.
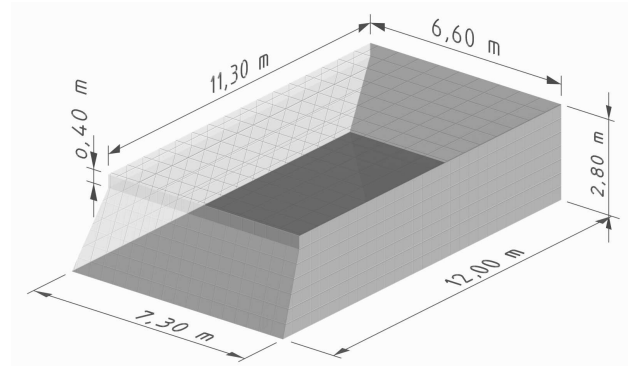

Figure 4: *Dimensions of the lecture hall T3 at Helsinki University of Technology, where reference response data was measured.*

The impulse response was recorded at 5.50 m from the left wall and 10.00 m from the front wall at a height of 1.70 m.

The hall was modeled using the 3-D triangular DWG mesh with junction spacing $\Delta x = 0.20$ m corresponding to $f_s = 2.875$ kHz. The simulation was run for 5000 time steps, which is equal to about 1.74 s. The reflection coefficients of the boundaries were approximated using two 3-tap FIR filters such as depicted in Fig. 3. One filter was used for the soft area of the ceiling, another for other surfaces. The filter coefficients R_1 and R_3 were bound to have equal values to make the filter linear phase. Thus there were 2 parameters to be optimized per filter. A Nelder-Mead optimization algorithm was run in Matlab to find the coefficients best matching with the mean T_{60} values measured on octave bands with central frequencies $62.5, 125, 250$, and 500 Hz. As the low-frequency cutoff of the sound source used for the measurements was at 69 Hz, there was no reliable data to match at lower frequencies.

The sums of the coefficients of each filter were bound to values below one to keep the simulation stable and the soft ceiling was bound to be more absorbing or equal with the other surfaces. The optimization was first done by hand and multiple runs of the optimization algorithm were tested with different starting values. The best results were obtained with $R_1 = R_3 = 0.019577$ and $R_2 = 0.8401$ for the hard surfaces and $R_1 = R_3 = 0.0089562$ and $R_2 = 0.85918$ for the ceiling. The resulting T_{60} values are listed in Table 1 and the simulated and measured responses are plotted with 5 Hz smoothing in Fig. 5. The reverberation times match fairly well, as do many of the peaks and the notches in the responses.

As a linear-phase filter was used, the wall locations were set only by the mesh size in increments of unit delays. This resulted in a good match with all dimensions for the floor and the ceiling, but the sloping walls could be modeled exactly only at certain heights. Also the height of the modeled space was overestimated by 0.08 m. With the fact that the lowered ceiling was not modeled as a separate boundary, this caused error in the simulated frequencies and magnitudes of the modes, seen as shifting of some peaks in Fig. 5. More detailed models could be built and the frequency-dependent reflection characteristics of the boundaries could be simulated more precisely using higher order filters.

Frequency / Hz	Measured T_{60} / s	Simulated T_{60} / s
62.5	1.62	1.44
125	1.23	1.41
250	0.75	0.64
500	0.67	0.50

Table 1: *Measured and simulated reverberation time values of the lecture hall T3 on four octave bands.*
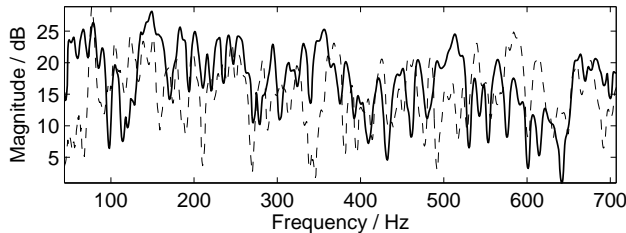

Figure 5: *Measured (−−) and simulated (—) responses of the lecture hall.*

6. CONCLUSIONS AND FUTURE WORK

A simplified structure for KW-conversion has been introduced. It saves computation, particularly if multiple K-ports are connected to a junction at an interface of the two variable types. The new KW-junction has been used in the special case of a mesh boundary, and a way of defining the reflection coefficients as a digital filter has been derived.

A second order linear-phase FIR-filter was used for modeling frequency-dependent reflection characteristics. Higher order filters are needed for more detailed control over the resulting reflection magnitude and phase. As a first addition, fractional delay could be utilised for fine-tuning the boundary locations. For directional reflection control, the boundary junction should be extended to having more than one port connected to the mesh. This kind of extension is also required, if the proposed boundary structure is to be used with the interpolated rectilinear mesh topology.

Finally, a large question that is out of the scope of this paper remains: What are the reflection and diffusion coefficient values of real surfaces at all frequencies and incident angles of interest? Good experimental results are essential for defining the filter characteristics for the simulated boundaries.

7. ACKNOWLEDGMENTS

8. REFERENCES

[1] M. R. Schroeder, "The "Schroeder frequency" revisited," *J. Acoust. Soc. Am.*, vol. 99, no. 5, pp. 3240–3241, May 1996.

[2] J. O. Smith, "Physical modeling using digital waveguides," *Computer Music J.*, vol. 16, no. 4, pp. 74–91, 1992.

[3] V. Välimäki, J. Pakarinen, C. Erkut, and M. Karjalainen, "Discrete-time modelling of musical instruments," *Reports on Progress in Physics*, vol. 69, no. 1, pp. 1–78, Jan. 2006.

[4] S. A. Van Duyne and J. O. Smith, "Physical modeling with the 2-D digital waveguide mesh," in *Proc. Int. Comp. Music Conf. (ICMC'93),* Tokyo, Japan, Sept. 1993, pp. 40–47.

[5] F. Fontana and D. Rocchesso, "Physical modeling of membranes for percussive instruments," *Acustica United with Acta Acustica*, vol. 84, pp. 529–542, May/June 1998.

[6] L. Savioja, T. Rinne, and T. Takala, "Simulation of room acoustics with a 3-D finite difference mesh," in *Proc. Int. Comp. Music Conf. (ICMC'94),* Århus, Denmark, Sept. 1994, pp. 463–466.

[7] S. A. Van Duyne and J. O. Smith, "The 3D tetrahedral digital waveguide mesh with musical applications," in *Proc. Int. Comp. Music Conf. (ICMC'96),* Hong Kong, Aug. 1996, pp. 9–16.

[8] P. Huang, S. Serafin, and J. O. Smith, "A waveguide mesh model for high-frequency violin body resonances," in *Proc. Int. Comp. Music Conf. (ICMC'00),* Berlin, Germany, Sept. 2000, pp. 86–89.

[9] J. Huopaniemi, L. Savioja, and M. Karjalainen, "Modeling of reflections and air absorption in acoustical spaces — a digital filter design approach," in *Proc. IEEE Workshop Appl. of Dig. Sig. Proc. to Audio and Acoust.,* New Palz, NY, Oct. 1997.

[10] M. J. Beeson and D. T. Murphy, "Virtual room modelling using hybrid digital waveguide mesh techniques," in *Proc. 147th Meeting Acoust. Soc. Am.,* New York, USA, vol. 115(5), May 2004, p. 2515, abstract.

[11] M. Karjalainen and C. Erkut, "Digital waveguides versus finite difference structures: Equivalence and mixed modeling," *EURASIP Journal on Applied Signal Processing*, vol. 7, pp. 978–989, June 2004.

[12] F. Fontana, D. Rocchesso, and E. Apollonio, "Using the waveguide mesh in modelling 3D resonators," in *Proc. COST-G6 Conf. on Digital Audio Effects (DAFx-00),* Verona, Italy, Dec. 2000, pp. 229–232.

[13] J. A. Laird, *The physical modelling of drums using digital waveguides*, ser. PhD Thesis. University of Bristol, Nov. 2001.

[14] S. A. Van Duyne and J. O. Smith, "The tetrahedral digital waveguide mesh," in *Proc. IEEE Workshop Appl. of Dig. Sig. Proc. to Audio and Acoust.,* New Palz, NY, Oct. 1995, pp. 234–237.

[15] L. Savioja and V. Välimäki, "Interpolated rectangular 3-D digital waveguide mesh algorithms with frequency warping," *IEEE Trans. Speech and Audio Proc.*, vol. 11, no. 6, pp. 783–790, Nov. 2003.

[16] G. R. Campos and D. M. Howard, "On the computational efficiency of different waveguide mesh topologies for room acoustic simulation," *IEEE Trans. Speech and Audio Proc.*, vol. 13, no. 5, pp. 1063 – 1072, Sept. 2005.

[17] L. Savioja, J. Huopaniemi, T. Lokki, and R. Väänänen, "Creating interactive virtual acoustic environments," *J. Audio Eng. Soc.*, vol. 47, no. 9, pp. 675–705, Sept. 1999.

[18] K. Lee and J. O. Smith, "Implementation of a highly diffusing 2-D digital waveguide mesh with a quadratic residue diffuser," in *Proc. Int. Comp. Music Conf. (ICMC'04),* Miami, USA, Nov. 2004, pp. 309–315.